

Geophysical Research Letters[®]



RESEARCH LETTER

10.1029/2023GL104379

Key Points:

- Quantitative paleohydraulic tools indicate that deep, low-sloping rivers were characteristic of 1.2 Ga Stoer Group
- Paleohydraulic data plot in the single-thread river planform regime in mechanistic frameworks for discriminating channel planform
- Field observations and theory indicate that the mud in bank sediments can provide sufficient cohesion to maintain deep flows

Supporting Information:

Supporting Information may be found in the online version of this article.

Correspondence to:

J. M. Valenza,
jvalenza@ucsb.edu

Citation:

Valenza, J. M., Ganti, V., Whittaker, A. C., & Lamb, M. P. (2023). Pre-vegetation, single-thread rivers sustained by cohesive, fine-grained bank sediments: Mesoproterozoic Stoer Group, NW Scotland. *Geophysical Research Letters*, 50, e2023GL104379. <https://doi.org/10.1029/2023GL104379>

Received 4 MAY 2023

Accepted 18 JUN 2023

Author Contributions:

Conceptualization: Jeffery M. Valenza, Vamsi Ganti, Alexander C. Whittaker, Michael P. Lamb

Data curation: Jeffery M. Valenza

Formal analysis: Jeffery M. Valenza, Vamsi Ganti, Alexander C. Whittaker

Investigation: Alexander C. Whittaker

Methodology: Jeffery M. Valenza, Vamsi Ganti, Alexander C. Whittaker, Michael P. Lamb

Resources: Vamsi Ganti, Alexander C. Whittaker

© 2023 The Authors.

This is an open access article under the terms of the [Creative Commons Attribution-NonCommercial License](#), which permits use, distribution and reproduction in any medium, provided the original work is properly cited and is not used for commercial purposes.

Pre-Vegetation, Single-Thread Rivers Sustained by Cohesive, Fine-Grained Bank Sediments: Mesoproterozoic Stoer Group, NW Scotland

Jeffery M. Valenza¹ , Vamsi Ganti^{1,2} , Alexander C. Whittaker³, and Michael P. Lamb⁴

¹Department of Geography, University of California Santa Barbara, Santa Barbara, CA, USA, ²Department of Earth Science, University of California Santa Barbara, Santa Barbara, CA, USA, ³Department of Earth Science and Engineering, Imperial College London, London, UK, ⁴Division of Geological and Planetary Sciences, California Institute of Technology, Pasadena, CA, USA

Abstract A Silurian shift in fluvial stratigraphic architecture, coincident with the appearance of terrestrial vegetation in the fossil record, is traditionally cited as evidence for exclusively shallow, braided planforms in pre-vegetation rivers. While recent recognition of deep, single-thread channels in pre-Silurian strata challenge this paradigm, it is unclear how these rivers maintained stable banks. Here, we reconstruct paleohydraulics and channel planform from fluvial cross-strata of the 1.2 Ga Stoer Group. These deposits are consistent with deep (4–7 m), low-sloping rivers (2.7×10^{-4} to 4.5×10^{-5}), similar in morphometry to modern single-thread rivers. We show that reconstructed bank shear stresses approximate the cohesion provided by sand-mud mixtures with 30%–45% mud—consistent with Stoer floodplain facies composition. These results indicate that sediment cohesion from mud alone could have fostered deep, single-thread, pre-vegetation rivers. We suggest that the Silurian stratigraphic shift could mark a kinematic change in channel migration rate rather than a diversification of planform.

Plain Language Summary The earliest appearance of rooted plant fossils coincides with widespread evidence of meandering rivers in the geologic record. This correlation has led researchers to suggest that meandering rivers only existed on our planet since terrestrial plants colonized the continents, and that pre-vegetation rivers were predominantly characterized by shallow and multi-thread channels. While there is growing evidence of deep, single-thread rivers predating the rise of land plants, it is currently unclear how these rivers maintained stable banks. Here, we combine observations of 1.2-billion-year-old river sediments in NW Scotland with mechanistic theories of river dune formation to constrain the geometry of pre-vegetation rivers. We show that our field observations are consistent with deposition by deep, low-sloping, and single-thread rivers, whose reconstructed geometry is similar to modern-day meandering, rather than braided, rivers. We also demonstrate that the mud fraction of the floodplain sediment could have provided sufficient cohesion to resist erosional forces in deep, low-sloping rivers. Together, our results indicate that single-thread rivers could have been prevalent before the rise of land plants, and that mud can provide sufficient bank strength for the development of deep rivers.

1. Introduction

Sedimentary strata record the numerous ways in which the evolution of life shaped our planet (Bowring et al., 1993; Davies et al., 2020; Fischer et al., 2016; Knoll & Carroll, 1999). One such event is the Silurian (~450 Ma) proliferation of terrestrial plants (Kenrick & Crane, 1997; Morris et al., 2018), which coincides with a global shift in fluvial stratigraphic architecture (Davies & Gibling, 2010; Gibling & Davies, 2012; Gibling et al., 2014; McMahan & Davies, 2018b). Historically, shallow, multi-thread flows (i.e., braided) were considered characteristic of all pre-vegetation rivers (Els, 1998; Gibling et al., 2014; Long, 1977; MacNaughton et al., 1997; Rainbird, 1992; S nderholm & Tirsgaard, 1998), in stark contrast to the predominance of single-thread, meandering planforms in modern alluvial rivers (Galeazzi et al., 2021). Rooted plants are hypothesized to have dramatically increased channel bank strength, decreased the ability of rivers to rework overbank deposits, and increased the production of mud through enhanced chemical weathering (Long, 1977; McMahan & Davies, 2018a)—all factors that promote channel stabilization and consequently the global dominance of single-thread river

Supervision: Vamsi Ganti, Alexander C. Whittaker

Validation: Michael P. Lamb

Visualization: Jeffery M. Valenza, Alexander C. Whittaker

Writing – original draft: Jeffery M. Valenza, Vamsi Ganti, Alexander C. Whittaker

Writing – review & editing: Jeffery M. Valenza, Vamsi Ganti, Alexander C. Whittaker, Michael P. Lamb

planforms. This hypothesis implies that the nature and pace of sediment, water, and biogeochemical routing and storage on continents underwent a unidirectional shift with the evolution of land plants.

Several lines of recent research have challenged this paradigm. First, quantification of Proterozoic channel-body dimensions has revealed a remarkable consistency in channel aspect ratios across the Proterozoic and Phanerozoic Eons (Ielpi et al., 2017). Second, observations of single-thread channel deposits in extraterrestrial environments (Lapôtre et al., 2019; Matsubara et al., 2015; Salese et al., 2020) and barren terrestrial landscapes (Ielpi, 2019; Ielpi & Lapôtre, 2018, 2020) indicate that vegetation is not required to restrict flow to a single thread. Third, paleohydraulic reconstructions of Neoproterozoic fluvial deposits indicate that some rivers achieved low gradients and deep flows, similar to modern continental rivers (Ganti et al., 2019). Finally, single-thread rivers have been replicated in physical experiments with fine sediment as the only cohesive agent (e.g., Peakall et al., 2007). Thus, the apparent Silurian shift in fluvial architecture has been hypothesized to represent a reduction in river channel migration rate, rather than a sudden diversification of river planform (Ganti et al., 2020; Ielpi & Lapôtre, 2020; Zeichner et al., 2021).

Despite the increasing recognition of planform variability in pre-Silurian rivers (Ganti et al., 2019; Ielpi et al., 2016; Ielpi & Rainbird, 2016; McMahon & Davies, 2020; Santos & Owen, 2016), it remains unclear how unvegetated channel banks were sufficiently stable to foster relatively deep channels, in which flow likely consistently exceeded the threshold stress of sediment motion (Ganti et al., 2019; Lapôtre et al., 2019). This knowledge gap, with an apparent domination of channel facies relative to floodplain facies in pre-Silurian fluvial strata, has led to the assumption that pre-vegetation, single-thread rivers were rare and/or limited to smaller streams (Davies et al., 2017, 2020; Long, 2011; McMahon & Davies, 2019). However, the documented ubiquity of river dunes in pre-Silurian deposits suggests the widespread existence of deep flows and stable channel banks before the rise of land plants (Ganti et al., 2019; Lapôtre et al., 2019).

Here, we combine geological observations of Mesoproterozoic fluvial deposits in NW Scotland and mechanistic theories of river dune formation to perform the earliest paleohydraulic reconstructions of terrestrial rivers. From these, we constrain channel geometries and planform and confirm that the Stoer Group hosts sedimentary structures consistent with deep, low-sloping, and single-thread rivers. Next, we constrain the threshold stress of erodibility of Stoer channel banks and identify the mud fraction required to stabilize channels into single-thread planforms. Finally, we show that floodplain sediments with a relatively modest mud fraction are capable of fostering deep, single-thread rivers in the absence of vegetation, consistent with field observations of Stoer Group floodplain strata.

2. Study Area

The Mesoproterozoic Stoer Group—interpreted as a succession of Laurentian rift basin deposits—is an exceptionally well-preserved sedimentary succession in NW Scotland (e.g., Lebeau et al., 2020; Parnell et al., 2011; Krabbendam, 2021; Stewart, 1982, 2002; Williams and Foden, 2011) (Figures 1a and 1b). Up to 2 km thick, it comprises conglomerates, sandstones, and mudstones with remarkably little metamorphic overprint (Ielpi et al., 2016; McMahon & Davies, 2018a; Stewart, 2002). Geochronological data constrain the depositional age to 1.2–1.1 Ga (Parnell et al., 2011; Turnbull et al., 1996) and paleomagnetic data indicate a paleolatitude of 10–30° N (Stewart, 2002). The Stoer Group lies unconformably over a basement of Lewisian Gneiss and is unconformably capped by the >6 km thick Torridon Group—the base of which is c. 1 Ga (e.g., Kinnaird et al., 2007; Krabbendam, 2021; Stewart, 2002).

The Stoer Group is divided into three formations: the basal Clachtoll Formation (CF), Bay of Stoer Formation (BSF) and Meall Dearg Formation (MDF). The CF comprises a range of lithofacies, beginning with basement-derived breccia-conglomerates, which appear to have filled paleovalleys. These are followed by trough cross-bedded sandstones representing river dune migration in subcritical flows alongside fine to medium-grained sandstones with parallel bedding and muddy sandstone facies (up to ~15% in matrix; Stewart (2002)). Desiccated red shales and siltstones with ripple-laminated fine sandstone beds (~3 m thick) have also been documented overlying and interfingering with trough cross-stratified facies (Ielpi et al., 2016).

The overlying BSF is dominated by trough cross-stratified, pebbly fluvial sandstones; planar-bedded sandstone constitutes a secondary facies, punctuated by cycles of muddy sandstones followed by shales (Stewart, 2002). Some of the finer-grained units of the CF and BSF have been interpreted as floodplain deposits ranging from sandy crevasse splays to muddy floodbasins (e.g., Ielpi, & Lapôtre, 2018; Ielpi et al., 2016). The BSF contains the famous Stac Fada member, interpreted to contain meteorite-impact ejecta and dated to $1,177 \pm 5$ Ma, which acts as a marker bed throughout the succession (Amor et al., 2008; Parnell et al., 2011). The BSF also contains the Poll a' Mhuilte member, which hosts lacustrine carbonates (Krabbendam, 2021). We did not sample these two members.

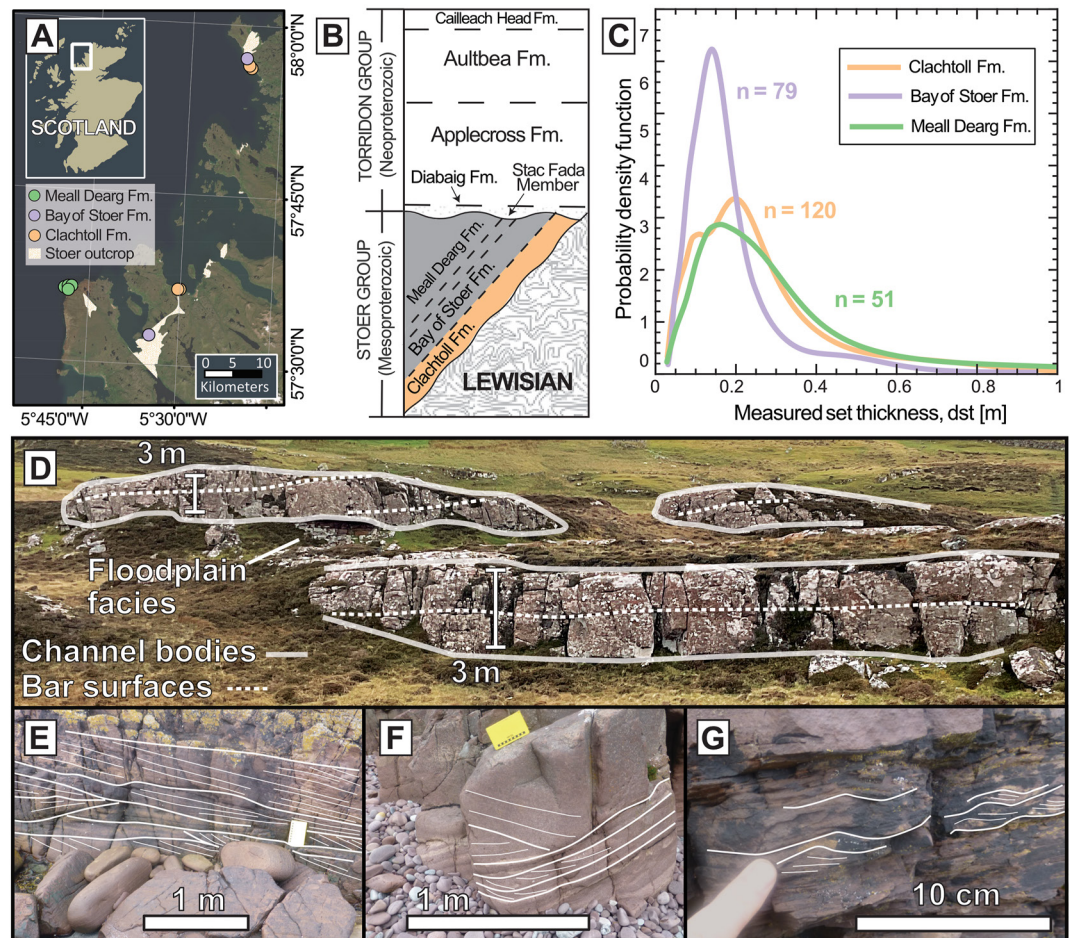


Figure 1. Outcrop and geologic background. (a) Distribution of study sites in NW Scotland. (b) Stratigraphic context of Mesoproterozoic Stoer Group, including the Clachtoll Formation (CF), Bay of Stoer Formation (BSF), and Meall Dearg Formation (MDF). (c) Dune cross-set thickness distributions measured from each of the three formations. (d) Outcrop character of channel bodies, CF, Stoer Peninsula, highlighting isolated channel bodies within poorly exposed floodplain facies. (e), (f) Example dune cross-stratification. (g) Observations of ripples in floodplain deposits of the CF.

The overlying MDF is dominated by fluvial facies associations, with minor aeolian strata (Lebeau & Ielpi, 2017; McMahon & Davies, 2018b). Fluvial facies include planar and trough cross-stratified medium-to-coarse sandstones and subordinate fine-to-medium rippled sandstones, mudstones, and desiccated shale drapes (Lebeau & Ielpi, 2017; Stewart, 2002). Antidune stratification, resulting from high-energy flood events, has also been reported (McMahon & Davies, 2018b).

Our work provides novel observations supporting a mechanistic explanation for the development of deep channels in the absence of vegetation. We built on the work of Ielpi et al. (2016), which documented channel-body and channel-belt architecture and demonstrated that the CF and BSF host deep channels within multi-story and/or multi-lateral channel belts. However, they did not quantify paleo-planform or potential controls on bank cohesion that led to the development of deep channels.

3. Materials and Methods

3.1. Field Observations and Published Data

We documented ripple, dune, and channel-scale features within the Stoer Group (Figure 1). We identified channel bodies as tabular or lensoidal sandstone packages isolated within fine-grained sediments (Figure 1d). Within channel-body features, we observed two distinct scales of bedform cross-set heights (thickness of bedform foreset package bounded by successive erosional boundaries), which we interpret as dune and bar deposits (Figure 1d).

We also observed preserved ripples in floodplain deposits and measured their wavelength for reconstruction of bank shear stress (Figure 1i; Section 3.4).

At the dune scale, we measured 138, 79, and 51 dune cross-set thicknesses, d_{st} , in the CF, BSF, and MDF, respectively (Figures 1e–1f, Data Set S1 in Supporting Information S1, Figure S1 in Supporting Information S1). We did not observe intra-formation trends in d_{st} , so we pooled data from each formation to characterize broad-scale behavior. We also observed sediment caliber and estimated the median grain size (D_{50}) of dune sets.

At the channel scale, we measured the aspect ratio of channel bodies in the CF and compiled channel-body thicknesses and widths reported by Ielpi et al. (2017) for the CF and BSF. The field localities of Ielpi et al. (2016, 2017) coincided with the locations where we made dune-scale field measurements. We also compiled mud-to-sand ratios of floodplain facies described in the CF and BSF (Ielpi et al., 2016). We compared paleohydraulic estimates with characteristics of modern channels described in the global compilation of Galeazzi et al. (2021).

3.2. Channel Geometry Reconstruction

In estimating channel geometry (flow depth and paleoslope), we propagated uncertainty by following established Monte Carlo methods for fluvial strata (Ganti et al., 2019; Lyster et al., 2021). We first generated 10^6 d_{st} values for each formation, using a two-parameter gamma distribution fit to observations (Figure 1c). To account for sediment compaction, we used a decompaction factor (D_f) range of 1.0–1.69 (Long, 2021). We generated 10^6 random, uniformly distributed D_f values to compute decompacted cross-set thicknesses (h_x) for each formation, where $h_x = D_f d_{st}$ (Table S1 in Supporting Information S1).

We estimated formative bedform heights (h_b) using a scaling relation derived from experiments and theory (Das et al., 2022; Ganti et al., 2013; Leclair & Bridge, 2001; Leclair et al., 2005; Paola & Borgman, 1991):

$$h_b = (2.9 \pm 0.7)h_x \quad (1)$$

Bridge (1997) suggested that Equation 1 is applicable so long as the coefficient of variation of h_x lies within the range of 0.58 and 1.28; we confirmed that h_x met this requirement for each formation (Table S1 in Supporting Information S1). To estimate h_b , we generated 10^6 values of the prefactor in Equation 1 using a normal distribution with mean and standard deviation (S.D.) of 2.9 and 0.7, respectively (Table S1 in Supporting Information S1).

We estimated formative flow depth using $H = 6.7h_b$ —an empirical relation based on experimental and field data (Bradley & Venditti, 2017). The first and third quartiles of the prefactor are 4.4 and 10.1, respectively (Bradley & Venditti, 2017), and we calculated an equivalent S.D. for the prefactor to propagate the uncertainty in h_b into estimates of H (Table S1 in Supporting Information S1).

The prevalence of dune cross-strata in the Stoer Group indicates that river dunes were stable during deposition. We leveraged empirically-derived relations between sediment transport and hydrodynamic conditions necessary for the stable existence of dunes to constrain riverbed slope, S (Ganti et al., 2019). Experimental and field observations outline the dimensionless Shields stress (τ^*) values under which dunes are stable for a given grain size (Lamb et al., 2012; Southard, 1991; van Rijn, 2007). Under the normal-flow approximation, paleoslope can be related to τ^* by definition as:

$$S = \frac{RD_{50}\tau^*}{H} \quad (2)$$

where R is the submerged specific density of sediment (1.65 for quartz). We used the bedform stability diagram of Lamb et al. (2012), which synthesizes a range of studies (van den Berg & van Gelder, 1993; Garcia, 2008; Southard & Boguchwal, 1990; Vanoni, 1974), to evaluate the τ^* range under which dunes are stable. We evaluated the upper and lower bounds on τ^* using estimated particle Reynolds numbers (Table S1, Figure S2 in Supporting Information S1), and generated 10^6 uniformly distributed random variables to evaluate the range of S values consistent with the stability of river dunes for each formation. We also estimated paleoslope using empirical scaling relations (Long, 2021; Trampush et al., 2014), independent of bedform stability, and found similar results (Figure S3b in Supporting Information S1). We preferred estimates of S based on bedform stability because it avoids bias from modern river data derived predominantly from single-thread channels.

3.3. Quantitative Assessment of Channel Planform

Given the complexities in identifying channel planform from fluvial stratigraphy (e.g., Best and Fielding (2019)), especially in sand-dominated systems (Hartley et al., 2015), we utilized mechanistic and empirical frameworks to assess channel planform. Parker (1976) showed that the development of braided planforms is driven by flow instabilities, and it occurs when $\frac{S}{Fr} \geq \frac{H}{W}$, where W is the width of the channel and Fr is the Froude number. Data from >550 modern rivers compiled by Lyster et al. (2022) confirmed the suitability of this approach for planform reconstruction. They then used empirical data to revise discriminant boundaries between planforms, suggesting that single-thread planforms exhibit $\frac{H}{W} \geq 0.02$, braided planforms exhibit $\frac{H}{W} < 0.02$ and $\frac{S}{Fr} > 0.003$, and anastomosing (wandering) planforms (multi-thread planform where new threads are formed predominantly through avulsion) exhibit $\frac{H}{W} < 0.02$ and $S/Fr \leq 0.003$.

To constrain H/W for Stoer Group channels, we used observations of isolated channel-body thicknesses and widths (aspect ratios; $n = 13$) within the CF (Figure 1d, Data Set S2 in Supporting Information S2), and aspect ratios ($n = 84$) measured by Ielpi et al. (2016, 2017) in the CF and BSF. In the absence of reported aspect ratios from the MDF, we apply those found in the CF and BSF. Furthermore, we consider these aspect ratios to indicate lower bounds of H/W , as actively migrating channels are typically a fraction of the width of resulting channel bodies (e.g., Hayden et al., 2019). Thus, our interpretations of river planform from estimated H/W are naturally biased toward multi-thread regimes. We validated the measured H/W using scaling relations presented by Long (2021) (Figures S3a and S3c in Supporting Information S1).

To constrain Fr in Equation 4, we assumed normal flow conditions and estimated the bed friction coefficient after Ma et al. (2022), which relates the bed friction coefficient to the ratio of shear velocity and sediment settling velocity (Figure S4 in Supporting Information S1). To test the validity of Equation 4 in describing modern data, we constrained H for the global compilation of rivers in Galeazzi et al. (2021) using empirical relations presented in Long (2021) and Fr using Manning's equation (Supporting Information S1).

3.4. Quantification of Bank Shear Stress

We constrained bank cohesion by estimating the shear stress applied on the banks for given channel dimensions. Lapôtre et al. (2019) relate the shear stress exerted on channel banks to bed shear stress of a single-thread river using a partitioning coefficient, ϵ :

$$\tau_{\text{bank}} = \epsilon \tau_{\text{bed}} \quad (3)$$

where $\tau_{\text{bed}} = \rho g H S$, and ρ is the density of water and g is the acceleration due to gravity. Assuming similar bed and wall roughness in a rectangular channel (Flintham & Carling, 1988; Knight et al., 1984), the partitioning coefficient is expressed as:

$$\epsilon = \frac{1.77 \left(\frac{W}{2H} \right)}{\left(\frac{W}{2H} + \frac{3}{2} \right)^{\frac{7}{5}} - 1.77} \quad (4)$$

Equations 3 and 4 provide an estimate of τ_{bank} and consequently the minimum cohesive strength of Stoer Group riverbanks. To estimate ϵ , we generated uniformly distributed H/W values between the lowest 25th percentile and highest 75th percentile values from field-measured datasets of channel-body aspect ratios.

We compared estimated τ_{bank} with the threshold stress of erodibility of sand-mud mixtures (Dunne & Jerolmack, 2022), using the observed mud fraction in floodplain facies of the CF and BSF (Dunne & Jerolmack, 2022; Ielpi et al., 2016, 2017). We also estimated the formative shear stress of well-preserved overbank ripples (Figure 1i), τ_{ripple} , as an additional constraint on τ_{bank} . Current ripples in proximal and levee settings are common during overbank flows, and physical experiments of fixed compound channels indicate that shear stress on floodplains can range from 20% to 60% of the shear stress exerted on channel banks and bed (e.g., Khatua and Patra (2007)). Thus, τ_{bank} can be a factor of 2–5 times greater than τ_{ripple} , where the latter can provide a lower bound on bank shear stress. Following Lapôtre et al. (2017), we estimated τ_{ripple} by solving for the bed shear

velocity ($\tau_{\text{ripple}} = \rho u_{\text{ripple}}^{*2}$), where u_{ripple}^* can be estimated from observations of median ripple grain size (D_{ripple}) and ripple wavelength (λ) (Figure 1i):

$$\lambda = 2504 \frac{\nu^{2/3} D_{\text{ripple}}^{1/6}}{(Rg)^{1/6} u_{\text{ripple}}^{*1/3}} \quad (5)$$

In Equation 5, ν is the kinematic viscosity of water (assumed to range between 8×10^{-7} – 1.3×10^{-6} m²/s, at 10–30°C). We propagated uncertainty into estimated τ_{ripple} by generating 10^6 uniformly distributed samples for each variable (λ , D_{ripple} , ν , and ρ).

4. Results

We observed 2–4 m thick isolated channel bodies with bar-scale cross-set thicknesses of 1–2 m in the CF (Figure 1d). These values were similar to the measured active channel-fill thicknesses in the BSF reported by Ielpi et al. (2016), which had a mean of 4.4 m. Measured dune cross-set thicknesses from the CF, BSF, and MDF had median values of 0.20 m ($n = 138$), 0.15 m ($n = 79$), and 0.27 m ($n = 51$), respectively (Figure 1c). The population mean cross-set thickness of each formation was significantly different (one-way ANOVA test, $P = 2.3 \times 10^{-5}$). The median grain sizes were 0.92, 1.5, and 0.35 mm for the CF, BSF, and MDF, respectively. The reconstructed median (interquartile range (IQR)) for dune bedform heights were 0.79 m (0.81 m), 0.62 m (0.51 m), and 1.06 m (1.11 m), and the reconstructed median (IQR) flow depths were 5.0 m (6.8 m), 4.0 m (4.7 m), and 6.6 m (9.2 m) for the CF, BSF, and MDF, respectively (Figure 2a). Using bedform stability diagrams, we estimated a median (IQR) S of 1.3×10^{-4} (2.3×10^{-4}), 2.7×10^{-4} (4.3×10^{-4}), and 4.5×10^{-5} (7.9×10^{-5}) for the CF, BSF, and MDF, respectively (Figure 2b)—values consistent with other empirical methods (Figure S3b in Supporting Information S1).

We interpreted Stoer Group river planforms using reconstructed hydraulics and geometries (Figure 2c). The channel-body aspect ratios, which we used as lower bound on H/W , reported by Ielpi et al. (2016, 2017) had a median (IQR) value of 0.015 (0.012) ($n = 84$), consistent with our estimated median (IQR) value of 0.09 (0.032) ($n = 13$; Data Set S2 in Supporting Information S2). The median (IQR) of the reconstructed S/Fr for the CF, BSF, and MDF was 1.1×10^{-3} (9.0×10^{-4}), 1.4×10^{-3} (1.1×10^{-3}), and 7.2×10^{-4} (5.8×10^{-4}), respectively (Figure 2c). Together, these values plot within the meandering regime of Parker (1976) (i.e., $S/Fr < H/W$) and align with the boundary between single-thread and anastomosing regimes of Lyster et al. (2022) (Figure 2c). A comparison of our reconstructed values with the global compilation of river planforms from Galeazzi et al. (2021) reinforces a meandering to high-sinuosity wandering planform interpretation for Stoer Group rivers (Figure 2c).

The median (IQR) of τ_{bank} for the Stoer Group rivers in the CF, BSF, and MDF was 4.3 (3.9) Pa, 7.0 (6.3) Pa and 1.9 (1.5) Pa, respectively (Figure 2d). Independent geologic evidence of floodplain ripples, including wavelengths of 8–12 cm and a median grain size range of coarse silt to very fine sand, indicates that τ_{bank} of Stoer Group rivers likely exceeded the reconstructed median (IQR) τ_{ripple} value of 1.3 (2.0) Pa (Figure 3). A comparison with experimental data of Dunne and Jerolmack (2022) suggests that the reconstructed τ_{bank} values correspond to threshold stresses of sand-mud mixtures with 30%–45% mud content (Figure 3a). Notably, this is similar to the reported clay content in Stoer muddy floodbasin facies of approximately 40% (Ielpi et al., 2016), which would yield an erodibility threshold of ~6 Pa (Figure 3a). Finally, we observed several exposures of muddy floodplain facies below and adjacent to channel bodies (Figures 1d and 3b). Together, these observations suggest that the cohesive strength of sand-mud mixtures found in Stoer Group floodplain sediments could plausibly foster deep, stable channels.

5. Discussion

Our results bolster a broadening recognition that pre-Silurian rivers commonly developed deep, single-thread channels (Ganti et al., 2019; Ielpi et al., 2016, 2022; Ielpi & Rainbird, 2015; Santos & Owen, 2016). These results depart from classical models ascribing shallow, braided planforms to pre-Silurian rivers as a rule (e.g., Cotter, 1977; Davies & Gibling, 2010; Gibling et al., 2014). Our results demonstrate that Mesoproterozoic Stoer Group rivers were characterized by deep (4–7 m) and low-sloping (4.5×10^{-5} to 2.7×10^{-4}) channels (Figures 2a and 2b), whose paleohydraulic characteristics were consistent with modern-day high-sinuosity, rather than braided, rivers (Figure 2c). These results are also consistent with observations of fluvial architecture from dune to channel scale. For example, Ielpi et al. (2016) reported dune-paleocurrent directions forming predominantly perpendicular to sub-perpendicular angles with bar-accretion surfaces, indicating high-sinuosity channels, and

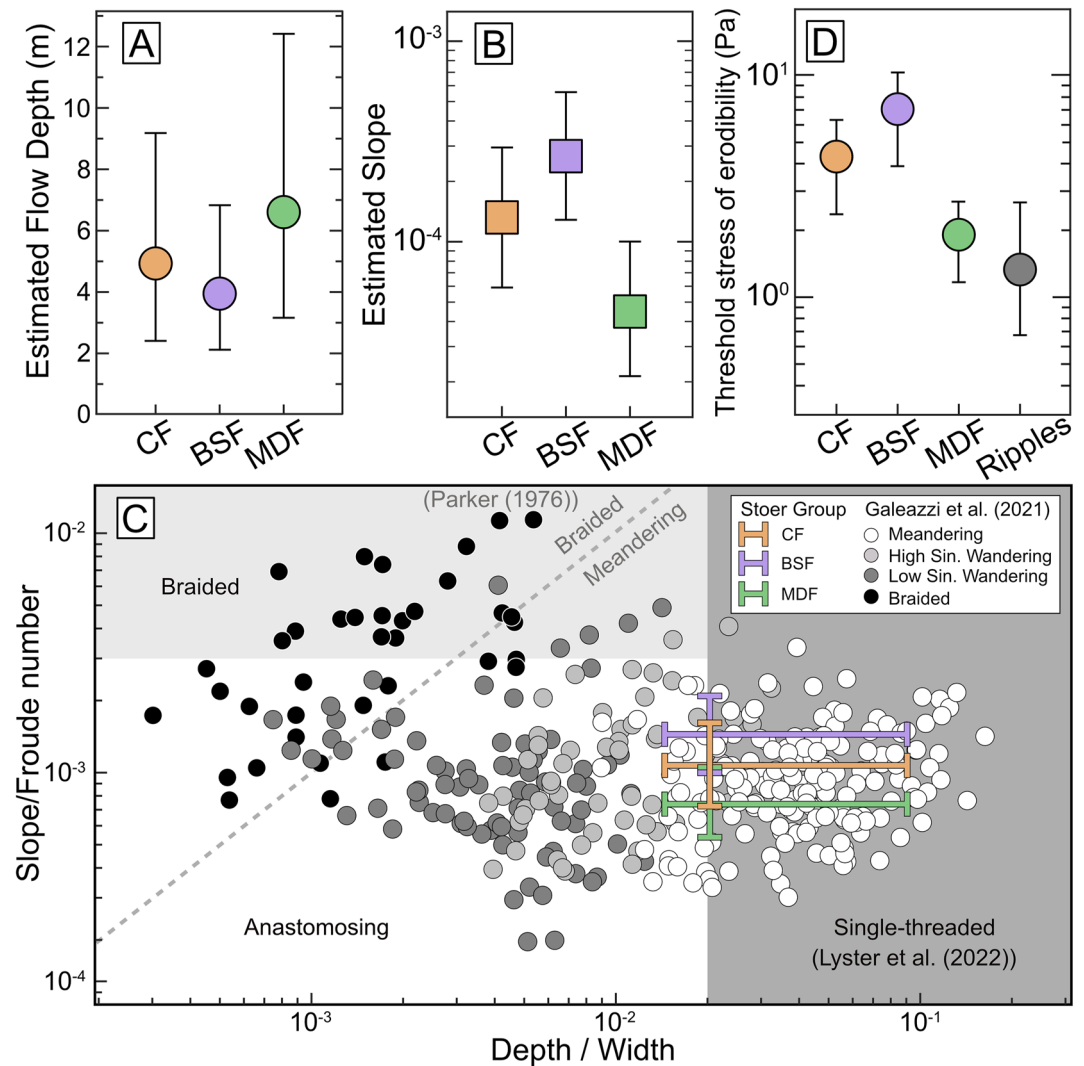


Figure 2. Reconstructed (a) flow depths and (b) riverbed slopes for Clachtoll Formation (orange), BSF (lavender), and MDF (green). (c) Channel planform discriminant space with reconstructed Stoeer Group data and a global compilation of modern rivers (circular markers; Galeazzi et al., 2021). The dashed line and various fields indicate the boundaries between different planforms proposed by Parker (1976) and Lyster et al. (2022), respectively. (d) Estimated threshold stress of erodibility, used as a proxy for bank cohesion. In all plots, the markers represent median values, and brackets denote interquartile ranges of variables.

we found that isolated channel-bodies within floodplain facies are a common feature of the CF (Figure 1d). Moreover, measured width-to-thickness ratios in the CF and BSF are consistent with deposits of mobile meandering rivers (Gibling et al., 2014) and our quantitative paleohydraulic analysis (Figure 2c).

Our work provides a mechanistic explanation for the widespread occurrence of deep flows in pre-vegetation Proterozoic rivers. Results from the Stoeer Group indicate that riverbanks could have been stabilized by the cohesion of sand-mud mixtures alone. Our analysis revealed that Stoeer Group channels supported median bank shear stresses in the range of 1.9–7.0 Pa (Figure 3a). These quantitative reconstructions were supported by observations of ripples in floodplain deposits (Figure 1g; Figure S4 in Supporting Information S1) that required 1.3 Pa of fluid shear stress for their formation during overbank flows (Figure 3a). Estimated bank cohesion values are consistent with experimental threshold shear stresses of sand-mud mixtures containing 30%–45% mud (Figure 3; Dunne & Jerolmack, 2022). Ielpi et al. (2016) reported 40% mud content in floodplain facies deposited by ephemeral ponds and occasionally deep overbank flows. Insofar as these facies are analogous to bank-toe material present in active channels, the observed floodplain material could then support stable channel banks. Indeed, we observed sharp contacts between sandy channel-fill packages and underlying muddy floodplain facies (e.g., Figure 3b). Together,

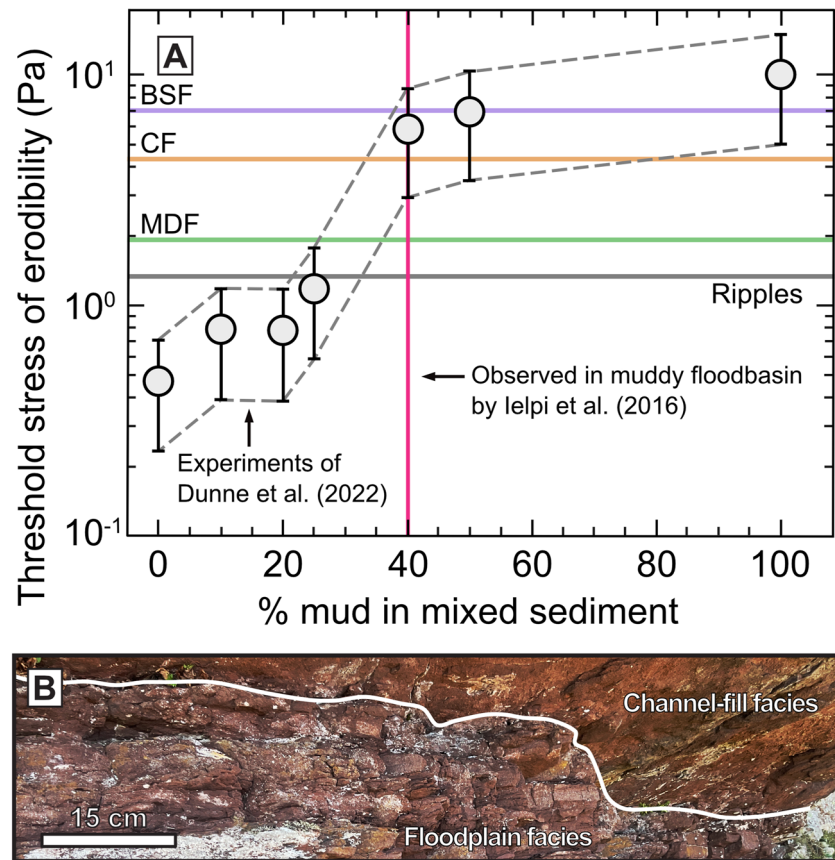


Figure 3. Threshold stress of erodibility of Stoer Group floodplain and bank sediments. (a) Median reconstructed bank shear stress for the CF, BSF, and MDF, and fluid stress for formation of ripples. Gray markers and confidence intervals indicate experimentally measured threshold stress of erodibility as a function of sediment composition (Dunne & Jerolmack, 2022). (b) Example contact between channel body (above) and floodplain heterolithics in the CF, Stoer Peninsula.

these results suggest that the mud content in predominantly sandy deposits, even in the absence of rooted vegetation, could foster deep, stable rivers in the Mesoproterozoic Era.

How can reconstructions of deep, stable pre-Silurian single-thread rivers be reconciled with the “sheet-braided” stratigraphic architecture often reported from Proterozoic fluvial systems? While some muddy floodplain deposits have been reported in the Stoer Group (e.g., Ielpi et al., 2016), deep flows have also been ascribed to the Neoproterozoic Torridon Group (Ganti et al., 2019) and Mesoproterozoic Burnside River Formation, Canada (Ielpi & Rainbird, 2016), in which muddy facies are rare. We suggest that the different facies associations reported from diverse deposits may indicate differences in fluvial kinematics and preservation, rather than planform (Ganti et al., 2020; Zeichner et al., 2021). Experimental work indicates that mud flocculation was likely facilitated by a synchronous increase in organic matter with the evolution of vascular plants, resulting in increasing mud deposition near channel margins (Zeichner et al., 2021)—a process that may have led to a slowdown in river migration. In addition, observations of elevated migration rates of channels from modern hyperarid systems suggests that rooted vegetation may also have led to a slowdown of channel migration in post-Silurian rivers (Ielpi & Lapôtre, 2020). The combination of decreased mud deposition near channel margins and higher migration rates may explain the common observation of heavily amalgamated channel facies, or “sheet-braided” architecture in pre-Silurian fluvial systems.

6. Conclusions

We combined original field observations of fluvial cross-strata from the Mesoproterozoic Stoer Group with mechanistic theories of the formation of river dunes to show:

1. Rivers that deposited Stoer Group sediments were characterized by deep flows (4–7 m), relatively low width-to-depth ratios, and low slopes (4.5×10^{-5} to 2.7×10^{-4}).

2. Reconstructed paleohydraulic data from the Stoer Group are consistent with modern meandering and high-sinuosity wandering rivers, and these data plot in the meandering planform discriminant space of Parker (1976) and along the threshold of meandering and anastomosing river regimes of Lyster et al. (2022).
3. Reconstructed median bank shear stresses (1.9–7.0 Pa) of Stoer Group rivers are consistent with the threshold of erodibility of sand-mud mixtures with 30%–45% mud content. This is consistent with observations of 40% mud content within Stoer Group floodplain facies.

In addition to these results, recent interpretations of stable, deep channels in other Proterozoic systems (Ganti et al., 2019; Ielpi & Rainbird, 2016) point to a previously unrecognized commonness of deep, single-thread rivers in the pre-Silurian period. We suggest that the mud content in these sediment transport systems could provide sufficient cohesion to sustain deep flows within stable channels, even if mud preservation was low in a stratigraphic context.

Data Availability Statement

All data, equations, sources, and methods (including unannotated photos, Figures S5 and S6 in Supporting Information S1) necessary to reproduce our results can be accessed in the following open-access repository: Dryad: <https://doi.org/10.25349/D9762J>.

References

- Amor, K., Hesselbo, S. P., Porcelli, D., Thackrey, S., & Parnell, J. (2008). A Precambrian proximal ejecta blanket from Scotland. *Geology*, 36(4), 303–306. <https://doi.org/10.1130/G24454A.1>
- Berg, J. H., & Gelder, A. (1993). A new bedform stability diagram, with emphasis on the transition of ripples to plane bed in flows over fine sand and silt. *Alluvial Sedimentation*, 11–21. <https://doi.org/10.1002/9781444303995.CH2>
- Best, J. I. M., & Fielding, C. R. (2019). Describing fluvial systems: Linking processes to deposits and stratigraphy. *Geological Society - Special Publications*, 488(1), 151–166. <https://doi.org/10.1144/SP488-2019-056>
- Bowring, S., Grotzinger, J., Isachsen, C., Knoll, A., Pelechaty, S., & Kolosov, P. (1993). Calibrating rates of early Cambrian evolution. *Science*, 261(5126), 1293–1298. <https://doi.org/10.1126/science.11539488>
- Bradley, R. W., & Venditti, J. G. (2017). Reevaluating dune scaling relations. *Earth-Science Reviews*, 165, 356–376. <https://doi.org/10.1016/j.earscirev.2016.11.004>
- Bridge, J. (1997). Thickness of sets of cross strata and planar strata as a function of formative bed-wave geometry and migration, and aggradation rate. *Geology*, 25(11), 971–974. [https://doi.org/10.1130/0091-7613\(1997\)025<0971:tosocs>2.3.co;2](https://doi.org/10.1130/0091-7613(1997)025<0971:tosocs>2.3.co;2)
- Das, D., Ganti, V., Bradley, R., Venditti, J., Reesink, A., & Parsons, D. R. (2022). The influence of transport stage on preserved fluvial cross strata. *Geophysical Research Letters*, 49(18). <https://doi.org/10.1029/2022GL099808>
- Davies, N. S., & Gibling, M. R. (2010). Cambrian to Devonian evolution of alluvial systems: The sedimentological impact of the earliest land plants. *Earth-Science Reviews*, 98(3–4), 171–200. <https://doi.org/10.1016/j.earscirev.2009.11.002>
- Davies, N. S., Gibling, M. R., McMahon, W. J., Slater, B. J., Long, D. G. F., Bashforth, A. R., et al. (2017). Discussion on “Tectonic and environmental controls on Palaeozoic fluvial environments: Reassessing the impacts of early land plants on sedimentation” *Journal of the Geological Society, London. Journal of the Geological Society*, 174(5), 947–950. <https://doi.org/10.1144/JGS2017-004>
- Davies, N. S., Shillito, A. P., Slater, B. J., Liu, A. G., & McMahon, W. J. (2020). Evolutionary synchrony of Earth's biosphere and sedimentary-stratigraphic record. *Earth-Science Reviews*, 201, 102979. <https://doi.org/10.1016/j.earscirev.2019.102979>
- Dunne, K. B. J., & Jerolmack, D. J. (2022). What sets river width? *Science Advances*, 6(41). <https://doi.org/10.1126/sciadv.abc1505>
- Els, B. G. (1998). The auriferous late Archaean sedimentation systems of South Africa: Unique palaeo-environmental conditions? *Sedimentary Geology*, 120(1–4), 205–224. [https://doi.org/10.1016/S0037-0738\(98\)00033-5](https://doi.org/10.1016/S0037-0738(98)00033-5)
- Fischer, W. W., Hemp, J., & Johnson, J. E. (2016). Evolution of oxygenic photosynthesis. <https://doi.org/10.1146/annurev-earth-060313-054810>
- Flintham, T. P., & Carling, P. A. (1988). The prediction of mean bed and wall boundary shear in uniform and compositely rough channels. In W. R. White (Ed.), *International conference on river regime* (pp. 267–287). John Wiley & Sons.
- Galeazzi, C. P., Almeida, R. P., & do Prado, A. H. (2021). Linking rivers to the rock record: Channel patterns and paleocurrent circular variance. *Geology*, 49(11), 1402–1407. <https://doi.org/10.1130/G49121.1>
- Ganti, V., Hajek, E. A., Leary, K., Straub, K. M., & Paola, C. (2020). Morphodynamic hierarchy and the fabric of the sedimentary record. *Geophysical Research Letters*, 47(14), e2020GL087921. <https://doi.org/10.1029/2020gl087921>
- Ganti, V., Paola, C., & Fofoula-Georgiou, E. (2013). Kinematic controls on the geometry of the preserved cross sets. *Journal of Geophysical Research: Earth Surface*, 118(3), 1296–1307. <https://doi.org/10.1002/JGRF.20094>
- Ganti, V., Whittaker, A. C., Lamb, M. P., & Fischer, W. W. (2019). Low-gradient, single-threaded rivers prior to greening of the continents. *Proceedings of the National Academy of Sciences of the United States of America*, 116(24), 11652–11657. <https://doi.org/10.1073/PNAS.1901642116>
- Garcia, M. (2008). In M. Garcia (Ed.), *Sedimentation engineering: Processes, measurements, modeling, and practice*. American Society of Civil Engineers. <https://doi.org/10.1061/9780784408148>
- Gibling, M. R., & Davies, N. S. (2012). Palaeozoic landscapes shaped by plant evolution. *Nature Geoscience*, 5(2), 99–105. <https://doi.org/10.1038/NNGEO1376>
- Gibling, M. R., Davies, N. S., Falcon-Lang, H. J., Bashforth, A. R., DiMichele, W. A., Rygel, M. C., & Ielpi, A. (2014). Palaeozoic co-evolution of rivers and vegetation: A synthesis of current knowledge. *Proceedings of the Geologists' Association*, 125(5–6), 524–533. <https://doi.org/10.1016/J.PGEOA.2013.12.003>
- Ielpi, A. (2019). Morphodynamics of meandering streams devoid of plant life: Amargosa River, Death Valley, California. *GSA Bulletin*, 131(5–6), 782–802. <https://doi.org/10.1130/B31960.1>

Acknowledgments

We thank Woody Fischer for useful discussions, and Tim Goudge and an anonymous reviewer for constructive comments. This work was supported by NSF Grants EAR 1935669 to Ganti and EAR-PF 2053029 to Valenza.

- Ielpi, A., & Lapôtre, M. (2018). Biotic forcing militates against river meandering in the modern Bonneville Basin of Utah. *Sedimentology*, 66(5), 1896–1929. <https://doi.org/10.1111/sed.12562>
- Ielpi, A., & Lapôtre, M. G. A. (2020). A tenfold slowdown in river meander migration driven by plant life. *Nature Geoscience*, 13(1), 82–86. <https://doi.org/10.1038/s41561-019-0491-7>
- Ielpi, A., & Rainbird, R. H. (2016). Highly variable Precambrian fluvial style recorded in the Nelson Head formation of Brock Inlier (Northwest Territories, Canada). *Journal of Sedimentary Research*, 86(3), 199–216. <https://doi.org/10.2110/jsr.2016.16>
- Ielpi, A., Rainbird, R. H., Ventra, D., & Ghinassi, M. (2017). Morphometric convergence between Proterozoic and post-vegetation rivers. *Nature Communications*, 8(1), 1–8. <https://doi.org/10.1038/ncomms15250>
- Ielpi, A., Ventra, D., & Ghinassi, M. (2016). Deeply channelled Precambrian rivers: Remote sensing and outcrop evidence from the 1.2 Ga Stoer Group of NW Scotland. *Precambrian Research*, 281, 291–311. <https://doi.org/10.1016/j.precamres.2016.06.004>
- Kenrick, P., & Crane, P. R. (1997). *The origin and early evolution of plants on land* (p. 389). Nature © Macmillan Publishers Ltd.
- Khatua, K., & Patra, K. (2007). Boundary shear stress distribution in compound open channel flow. *ISH Journal of Hydraulic Engineering*, 13(3), 39–54. <https://doi.org/10.1080/09715010.2007.10514882>
- Kinnaird, T. C., Prave, A. R., Kirkland, C. L., Horstwood, M., Parrish, R., & Batchelor, R. A. (2007). The late Mesoproterozoic—early Neoproterozoic tectonostratigraphic evolution of NW Scotland: The Torridonian revisited. *Journal of the Geological Society*, 164, 541–551. <https://doi.org/10.1144/0016-76492005-096>
- Knight, D. W., Demetriou, J. D., & Hamed, M. E. (1984). Stage discharge relationships for compound channels. In K. V. H. Smith (Ed.), *Channels and channel control structures* (pp. 445–459). Springer-Verlag.
- Knoll, A. H., & Carroll, S. B. (1999). Early animal evolution: Emerging views from comparative biology and geology. *Science*, 284, 2129–2137. <https://doi.org/10.1126/science.284.5423.2129>
- Krabbenham, M. (2021). *A stratigraphic framework for the early Neoproterozoic successions of the Northern Highlands of Scotland*. UK Stratigraphic Framework Series National Geoscience Programme.
- Lamb, M. P., Grotzinger, J. P., Southard, J. B., & Tosca, N. J. (2012). Were aqueous ripples on Mars formed by flowing brines? *SEPM Special Publications*, 102, 139–150. <https://doi.org/10.2110/PEC.12.102.0139>
- Lapôtre, M. G. A., Ielpi, A., Lamb, M. P., Williams, R. M. E., & Knoll, A. H. (2019). Model for the formation of single-thread rivers in barren landscapes and implications for pre-Silurian and Martian fluvial deposits. *Journal of Geophysical Research: Earth Surface*, 124(12), 2757–2777. <https://doi.org/10.1029/2019JF005156>
- Lapôtre, M. G. A., Lamb, M. P., & McElroy, B. (2017). What sets the size of current ripples? *Geology*, 45(3), 243–246. <https://doi.org/10.1130/G38598.1>
- Lebeau, L. E., & Ielpi, A. (2017). Fluvial channel-belts, floodbasins, and Aeolian ergs in the Precambrian Meall Dearg Formation (Torridonian of Scotland): Inferring climate regimes from pre-vegetation clastic rock records. *Sedimentary Geology*, 357, 53–71. <https://doi.org/10.1016/j.sedgelo.2017.06.003>
- Leclair, S. F., Blom, A., Michael, V., Blum, D., & Marriott, S. B. (2005). A qualitative analysis of the distribution of bed-surface elevation and the characteristics of associated deposits for subaqueous dunes. *Special Publication of the International Association of Sedimentologists*, 35, 121–134. <https://doi.org/10.1002/9781444304350.ch7>
- Leclair, S. F., & Bridge, J. S. (2001). Quantitative interpretation of sedimentary structures formed by river dunes. *Journal of Sedimentary Research*, 71(5), 713–716. <https://doi.org/10.1306/2DC40962-0E47-11D7-8643000102C1865D>
- Long, D. G. F. (1977). Proterozoic stream deposits: Some problems of recognition and interpretation of ancient sandy fluvial systems. *Fluvial Sedimentology -- Memoirs*, 5, 313–341.
- Long, D. G. F. (2011). Architecture and depositional style of fluvial systems before land plants: A comparison of Precambrian, early Paleozoic, and modern river deposits. In *From River to Rock Record: The preservation of fluvial sediments and their subsequent interpretation* (Vol. 97, pp. 37–62). SEPM Society for Sedimentary Geology. <https://doi.org/10.2110/SEPMSP.097.037>
- Lyster, S. J., Whittaker, A. C., & Hajek, E. A. (2022). The problem of paleo-planforms. *Geology*, 50(7), 822–826. <https://doi.org/10.1130/G49867.1>
- Ma, H., Nittrouer, J. A., Fu, X., Parker, G., Zhang, Y., Wang, Y., et al. (2022). Amplification of downstream flood stage due to damming of fine-grained rivers. *Nature Communications*, 13(1), 1–11. <https://doi.org/10.1038/s41467-022-30730-9>
- MacNaughton, R. B., Dalrymple, R. W., & Narbonne, G. M. (1997). Early Cambrian braid-delta deposits, MacKenzie Mountains, north-western Canada. *Sedimentology*, 44(4), 587–609. <https://doi.org/10.1046/j.1365-3091.1997.D01-41.x>
- Matsubara, Y., Howard, A. D., Burr, D. M., Williams, R. M. E., Dietrich, W. E., & Moore, J. M. (2015). River meandering on Earth and Mars: A comparative study of Aeolis dorsa meanders, Mars and possible terrestrial analogs of the Usumtuk river, AK, and the Quinn river, NV. *Geomorphology*, 240, 102–120. <https://doi.org/10.1016/j.geomorph.2014.08.031>
- McMahon, W. J., & Davies, N. S. (2018a). Evolution of alluvial mudrock forced by early land plants. *Science*, 359(6379), 1022–1024. <https://doi.org/10.1126/science.aan4660>
- McMahon, W. J., & Davies, N. S. (2018b). High-energy flood events recorded in the Mesoproterozoic Meall Dearg Formation, NW Scotland: their recognition and implications for the study of pre-vegetation alluvium. *Journal of the Geological Society*, 175(1), 13–32. <https://doi.org/10.1144/JGS2017-012>
- McMahon, W. J., & Davies, N. S. (2019). The shortage of geological evidence for pre-vegetation meandering rivers. In M. Ghinassi, L. Colombera, N. P. Mountney, & A. J. Reesink (Eds.), *Fluvial meanders and their sedimentary products in the rock record* (1st ed., Vol. 48, pp. 119–148). John Wiley & Sons. <https://doi.org/10.1002/9781119424437.ch5>
- McMahon, W. J., & Davies, N. S. (2020). Physical and biological functioning in Proterozoic rivers: Evidence from the archetypal pre-vegetation alluvium of the Torridon Group, NW Scotland. *Scottish Journal of Geology*, 56, 1–29. <https://doi.org/10.1144/sjg2019-013>
- Morris, J. L., Puttick, M. N., Clark, J. W., Edwards, D., Kenrick, P., Pressel, S., et al. (2018). The timescale of early land plant evolution. *Proceedings of the National Academy of Sciences of the United States of America*, 115(10), E2274–E2283. <https://doi.org/10.1073/pnas.1719588115>
- Paola, C., & Borgman, L. (1991). Reconstructing random topography from preserved stratification. *Sedimentology*, 38(4), 553–565. <https://doi.org/10.1111/j.1365-3091.1991.tb01008.x>
- Parker, G. (1976). On the cause and characteristic scales of meandering and braiding in rivers. *Journal of Fluid Mechanics*, 76(3), 457–480. <https://doi.org/10.1017/S00222112076000748>
- Parnell, J., Mark, D., Fallick, A. E., Boyce, A., & Thackrey, S. (2011). The age of the Mesoproterozoic Stoer Group sedimentary and impact deposits, NW Scotland. *Journal of the Geological Society*, 168, 349–358. <https://doi.org/10.1144/0016-76492010-099>
- Peakall, J., Ashworth, P. J., & Best, J. L. (2007). Meander-bend evolution, alluvial architecture, and the role of cohesion in sinuous river channels: A flume study. *Journal of Sedimentary Research*, 77(3), 197–212. <https://doi.org/10.2110/jsr.2007.017>

- Rainbird, R. (1992). Anatomy of a large-scale braid-plain quartzarenite from the Neoproterozoic Shaler Group, Victoria Island, Northwest Territories, Canada. *Canadian Journal of Earth Sciences*, 29(12), 2537–2550. <https://doi.org/10.1139/e92-201>
- Salese, F., McMahon, W. J., Balme, M. R., Ansan, V., Davis, J. M., & Kleinhans, M. G. (2020). Sustained fluvial deposition recorded in Mars' Noachian stratigraphic record. *Nature Communications*, 11(1), 2067. <https://doi.org/10.1038/s41467-020-15622-0>
- Santos, M. G. M., & Owen, G. (2016). Heterolithic meandering-channel deposits from the Neoproterozoic of NW Scotland: Implications for palaeogeographic reconstructions of Precambrian sedimentary environments. *Precambrian Research*, 272, 226–243. <https://doi.org/10.1016/j.precamres.2015.11.003>
- Sønderholm, M., & Tirsgaard, H. (1998). Proterozoic fluvial styles: Response to changes in accommodation space (Rvieradal sandstones, eastern north Greenland). *Sedimentary Geology*, 120(1–4), 257–274. [https://doi.org/10.1016/S0037-0738\(98\)00035-9](https://doi.org/10.1016/S0037-0738(98)00035-9)
- Southard, J. B. (1991). Experimental determination of bed-form stability. *Annual Review of Earth and Planetary Sciences*, 19(1), 423–455. <https://doi.org/10.1146/ANNUREV.EA.19.050191.002231>
- Southard, J. B., & Boguchwal, L. A. (1990). Bed configurations in steady unidirectional water flows. Part 2. Synthesis of flume data. *Journal of Sedimentary Petrology*, 60(5), 658–679. <https://doi.org/10.1306/212F9241-2B24-11D7-8648000102C1865D>
- Stewart, A. D. (2002). *The later Proterozoic Torridonian rocks of Scotland: Their sedimentology, geochemistry and origin. The Geological Society of London—Memoirs*, 24. <https://doi.org/10.1144/GSL.MEM.2002.024>
- Turnbull, M. M., Whitehouse, M. J., & Moorbath, S. (1996). New isotopic age determinations for the Torridonian, NW Scotland. *Journal of the Geological Society*, 153(6), 955–964. <https://doi.org/10.1144/gsjgs.153.6.0955>
- Vanoni, V. A. (1974). Factors determining bed forms of alluvial streams. *Journal of the Hydraulics Division*, 100(3), 363–377. <https://doi.org/10.1061/JYCEAJ.0003906>
- van Rijn, L. C. (2007). Unified view of sediment transport by currents and waves. I: Initiation of motion, bed roughness, and bed-load transport. *Journal of Hydraulic Engineering*, 133(6), 649–667. [https://doi.org/10.1061/\(asce\)0733-9429\(2007\)133:6\(649\)](https://doi.org/10.1061/(asce)0733-9429(2007)133:6(649))
- Williams, G. E., & Foden, J. (2011). A unifying model for the Torridon Group (early Neoproterozoic), NW Scotland: Product of post-Grenvillian extensional collapse. *Earth-Science Reviews*, 108(1–2), 34–49. <https://doi.org/10.1016/j.earscirev.2011.05.004>
- Zeichner, S. S., Nghiem, J., Lamb, M. P., Takashima, N., de Leeuw, J., Ganti, V., & Fischer, W. W. (2021). Early plant organics increased global terrestrial mud deposition through enhanced flocculation. *Science*, 371(6528), 526–529. <https://doi.org/10.1126/science.abd0379>

References From the Supporting Information

- Arcement, G. J., & Schneider, V. R. (1989). *Guide for selecting Manning's roughness coefficients for natural channels and flood plains*. USGS Water-Supply.
- Cotter, E. (1977). *The evolution of fluvial style, with special reference to the central Appalachian Paleozoic* (Vol. 5, pp. 361–383). *Fluvial Sedimentology—Memoirs*, 5. Retrieved from http://archives.datapages.com/data/dgs/005/005001/361_cspgsp0050361.htm
- Engelund, F., & Hansen, E. (1967). A monograph on sediment transport in alluvial streams. Technical University of Denmark Østervoldgade 10, Copenhagen K.
- Ferguson, R., & Church, M. (2004). A simple universal equation for grain settling velocity. *Journal of Sedimentary Research*, 74(6), 933–937. <https://doi.org/10.1306/051204740933>
- Hartley, A. J., Owen, A., Swan, A., Weissmann, G. S., Holzweber, B. I., Howell, J., et al. (2015). Recognition and importance of amalgamated sandy meander belts in the continental rock record. *Geology*, 43(8), 679–682. <https://doi.org/10.1130/G36743.1>
- Hayden, A. T., Lamb, M. P., Fischer, W. W., Ewing, R. C., McElroy, B. J., & Williams, R. M. E. (2019). Formation of sinuous ridges by inversion of river-channel belts in Utah, USA, with implications for Mars. *Icarus*, 332, 92–110. <https://doi.org/10.1016/j.icarus.2019.04.019>
- Ielpi, A., Lapotre, M. G., Gibling, M. R., & Boyce, C. K. (2022). The impact of vegetation on meandering rivers. *Nature Reviews Earth & Environment*, 3, 165–178. <https://doi.org/10.1038/s43017-021-00249-6>
- Ielpi, A., & Rainbird, R. H. (2015). Architecture and morphodynamics of a 1.6 Ga fluvial sandstone: Ellice formation of Elu basin, arctic Canada. *Sedimentology*, 62(7), 1950–1977. <https://doi.org/10.1111/sed.12211>
- Lebeau, L. E., Ielpi, A., Krabbendam, M., & Davis, W. J. (2020). Detrital-zircon provenance of a Torridonian fluvial-Aeolian sandstone: The 1.2 Ga Meall Dearg Formation, stoe Group (Scotland). *Precambrian Research*, 346, 105822. <https://doi.org/10.1016/j.precamres.2020.105822>
- Long, D. G. F. (2021). Trickle down the paleoslope: An empirical approach to paleohydrology. *Earth-Science Reviews*, 220, 103740. <https://doi.org/10.1016/j.earscirev.2021.103740>
- Lyster, S. J., Whittaker, A. C., Hampson, G. J., Hajek, E. A., Allison, P. A., & Lathrop, B. A. (2021). Reconstructing the morphologies and hydrodynamics of ancient rivers from source to sink: Cretaceous Western Interior Basin, Utah, USA. *Sedimentology*, 68(6), 2854–2886. <https://doi.org/10.1111/SED.12877>
- Stewart, A. D. (1982). Late Proterozoic rifting in NW Scotland: The Genesis of the “torridonian”. *Journal of the Geological Society of London*, 139(4), 413–420. <https://doi.org/10.1144/gsjgs.139.4.0413>
- The MathWorks Inc. (2022). *Curve fitter toolbox version 3.8 (R2022b)*. The MathWorks Inc. Retrieved from <https://www.mathworks.com>
- Trampush, S. M., Huzurbazar, S., & McElroy, B. (2014). Empirical assessment of theory for bankfull characteristics of alluvial channels. *Water Resources Research*, 50(12), 9211–9220. <https://doi.org/10.1002/2014WR015597>